Journal of Vegetation Science **23** (2012) 406–418

A novel method for extracting green fractional vegetation cover from digital images

Yaokai Liu, Xihan Mu, Haoxing Wang & Guangjian Yan

Keywords
Colour space; Digital photography; Fractional vegetation cover; Gaussian model; Image segmentation

Received 8 May 2011
Accepted 24 October 2011
Co-ordinating Editor: Geoffrey Henebry

Mu, X. (corresponding author, muxihan@bnu.edu.cn, hiker_liu@163.com), **Liu, Y.** (hiker_liu@163.com) & **Yan, G.** (gjyan@bnu.edu.cn): State Key Laboratory of Remote Sensing Science, Beijing Key Laboratory for Remote Sensing of Environment and Digital Cities, School of Geography, Beijing Normal University, Beijing, 100875, China
Liu, Y. (hiker_liu@163.com): Academy of Opto-Electronics, Chinese Academy of Sciences, Beijing, 100094, China
Wang, H. (wang_haox@mail.bnu.edu.cn): Institute of Automation, Chinese Academy of Sciences, Beijing, 100029, China

Abstract

Question: Although digital photography is an efficient and objective means of extracting green fractional vegetation cover (FVC), it lacks automation and classification accuracy. How can green FVC be extracted from digital images in an accurate and automated method?

Methods: Several colour spaces were compared on the basis of a separability index, and CIE $L^*a^*b^*$ was shown to be optimal for the tested colour spaces. Thus, all image processing was performed in CIE $L^*a^*b^*$ colour space. Gaussian models were used to fit the green vegetation and background distributions of the a^* component. Three strategies (T_0, T_1 and T_2 thresholding method) were tested to select the optimal thresholds for segmenting the image into green vegetation and non-green vegetation. The a^* components of the images were then segmented and the green FVC extracted.

Results: The FVC extracted using T_0, T_1, and T_2 thresholding methods were evaluated with simulated images, and cross-validated with FVC extracted with supervised classification methods. The results show that FVC extracted with T_0, T_1 and T_2 thresholding methods are similar to those estimated with supervised classification methods. The mean errors associated with the FVC values provided in our approach and supervised classification are less than 0.035. In a test with simulated data, our method performed better than the supervised classification method.

Conclusions: Methods presented in this paper were demonstrated to be feasible and applicable for automatically and accurately extracting FVC of several green vegetation types with varying background and shadow conditions. However, our algorithm design assumes a Gaussian distribution for both vegetated and non-vegetated portions of a digital image; moreover, the impact of view angle on the FVC extraction from digital images must also be considered.

Introduction

Fractional vegetation cover (FVC) is defined as the percentage of vegetation occupying a unit area. It accounts for the fraction of vegetation on a flat background covered with vegetation. Vegetation plays an essential role in the exchange of carbon, water and energy at the land surface (Tueller 1987; Choudhury 1994; Nemani & Running 1996; Hoffmann & Jackson 2000; Schimel et al. 2001). Estimated FVC is often required for modelling vegetation productivity and studies related to land surfaces, climatology, hydrology, ecology and agricultural resource management (Prince 1991; Sellers et al. 1997; McVicar & Jupp 1998; Gower et al. 1999; Qi et al. 2000; Behrenfeld et al. 2001). Since its initial development, remote sensing has become the primary method got estimating the fractions of vegetation cover. However, estimates made from remote sensing images must be validated with on-the-ground truth data, especially when the estimates will be used for further study of vegetation modelling and monitoring (Zhou et al. 1998).

A number of conventional field measurements can be made to obtain the true FVC. Adams & Arkin (1977) described a meter-stick method for measuring ground cover of row crops and compared it with several other methods, such as SQS (spatial quantum sensor) and TQS (traversing quantum sensor) methods, concluding that the meter-stick method was the simplest, most

Doi: 10.1111/j.1654-1103.2011.01373.x

economical and fastest method, and was also as accurate as any other method of measuring ground cover. Dymond et al. (1992) used a quadrat method to determine the actual vegetation cover of degraded rangeland, which was used to validate the ground cover estimate from SPOT data. The point-count method has been used along random transects; the percentage of cover is calculated as the percentage of green leaf counts per total number of counts in the measured transects (Elvidge & Chen 1995). Kercher et al. (2003) evaluated variability in cover estimation data obtained by two sampling teams who double-sampled plots. Vittoz et al. (2010) also assessed the variability of multiple records of plant species cover from the same spatial units using several common methods; however, some of these methods are subjective and cannot be conveniently implemented. Zhou et al. (1998) compared a number of ground sampling methods for quantitative vegetation cover estimation and argued that the results are often inconsistent and unreliable. Zhou & Robson (2001) suggested that an ideal ground investigation method for estimating rangeland vegetation cover should: (1) employ cost-efficient and easy-to-use field equipment; (2) record accurate and objective field observations; (3) place minimum demands on field time; and (4) derive the required parameters with minimum interference from human operators.

During recent decades, many studies have focused on the separation of green vegetation from background soil in digital photography by means of computer analysis techniques (Brown et al. 2000; Zhou & Robson 2001; Leblanc et al. 2005; Macfarlane et al. 2007; Gallegos & Glimskar 2009; Baret et al. 2010; Liu & Pattey 2010).

Although digital photography is an efficient, accurate and objective means of extracting green FVC, it lacks automation and classification accuracy. Early methods of extracting quantitative information from photographs used stereographic pairs and a human interpreter to extract information (Wimbush et al. 1967; Wells 1971). Human interpretation has also been used to estimate green FVC by selecting vegetation samples from digital images (Brogaard & Ólafsdóttir 1997; Zhou et al. 1998). More recently, digital image analysis has been combined with supervised and unsupervised classification methods to determine FVC, but unfortunately these methods usually produce inaccurate results and are time-consuming (Zhou & Robson 2001). Various image segmentation approaches have been used to extract green vegetation or gap fractions from digital photographs under different scenarios. Andreasen et al. (1997) defined a parameter for separating plants from soil in red–green–blue (RGB) colour images as $g = 256(G/(R + G + B))$. Booth et al. (2006) used a 'green leaf' algorithm $((G-R) + (G-B))/(G + R + G + B)$ to detect positive values, which are indicative of green vegetation because they contain higher green levels than red or blue levels (Louhaichi et al. 2001). Demarez et al. (2008) calculated the gap fraction from RGB images using a supervised classification method that can be used estimate FVC. Graham et al. (2009) used hue, saturation and lightness (HSL) colour space to segment green vegetation from background data. Baret and colleagues (2010) proposed a technique to estimate the green area index of row crops using the RGB colour space from downward-looking digital photos. Liu & Pattey (2010) used greenness (2G−R−B) for the image segmentation to extract gap fractions from digital photographs.

The purpose of this study is to develop an automated green FVC extraction system for synoptic digital imagery that has a high degree of analytical accuracy. The new method is verified by comparing results obtained using it to those obtained using supervised and unsupervised classification methods, as well as the 2G−R−B reference method of Liu & Pattey (2010).

Methods

Site description and data acquisition for the field experiment

The study was conducted from June to September 2010 at the Huailai Experiment Station, about 80 km north of Beijing (40° 20′57″ N, 115° 47′03″ E). Maize is the main crop in the study area, along with some cash crops such as grapevine, peanut and peach.

Our field experiments coincided with the growth cycle of maize, beginning on 05.06.2010 and ending on 26.09.2010. Digital images were acquired at nadir at a height of 3 m above the ground and were taken with a Nikon D3000 camera, mounted on a simple observation platform. The images were obtained via remote control and were stored in the JPGE format with a size of 3872 by 2592 pixels. Because of distortion from the central projection of the digital camera, the edges of the images were cropped, reducing the size to 1739 by 1739 pixels.

Employing a Gaussian model and fitting data to the Gaussian curve

Most digital images are stored in three dimensions using RGB colour space. One advantage of colour photographs is their ability to capture a greater variety of situations, especially in outdoor scenes (Philipp & Rath 2002). For FVC extraction, colour images offer more dimensions for image segmentation. However, in practice, the classification of green vegetation and background is achieved by determining a threshold T_0 in one-dimensional space (see Fig. 1),

Doi: 10.1111/j.1654-1103.2011.01373.x

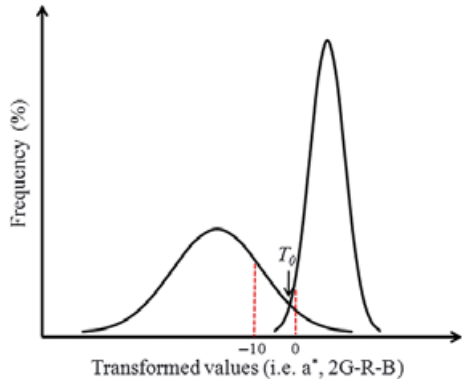

Fig. 1. Distribution curves for vegetation and background showing how the T_0 threshold for segmenting images falls below 0. The curves are based on Gaussian distribution and represent the transformed values after the image has been transformed from RGB to other colour space.

which is formed as a combination of RGB channels or components of other colour spaces (e.g. $L^*a^*b^*$ or i1i2i3; Philipp & Rath 2002). The distributions of the vegetation and background transformed from RGB digital images were assumed to follow Gaussian distributions, and the following functions can be used to analyse the distributions of the transformed values:

$$F(x) = \frac{w_1}{\sqrt{2\pi}\sigma_1} e^{-\frac{(x-\mu_1)^2}{2\sigma_1^2}} + \frac{w_2}{\sqrt{2\pi}\sigma_2} e^{-\frac{(x-\mu_2)^2}{2\sigma_2^2}} \qquad (1)$$

where μ_1 and μ_2 are the means of the green vegetation and the background, respectively; σ_1 and σ_2 are the standard deviations of the green vegetation and the background, respectively; and w_1 and w_2 are the weights of the green vegetation and the background, respectively.

A curve-fitting method was used to obtain the parameters in Eq. (1) for the distributions of vegetation and background components. First, a sensitive region of the threshold was chosen experimentally, then the value with minimum frequency in the sensitive region was established as the initial threshold to segment the digital image into vegetation and background. The distribution of each part obeys Gaussian distribution. Finally, two Gaussian curves were used to fit these two segments to obtain the parameters of the Gaussian models.

Selecting an optimal colour space

The detection of objects in digital images is often achieved by applying a thresholding operation to the three-dimensional RGB colour space. This can take a number of forms, such as (R + G + B)/3, R−B, (2G−R−B)/2, and 2G−R−B. All of the forms are transformed from RGB colour space and have all been used to segment digital images (Ohta et al. 1980; Woebbecke et al. 1995; Liu & Pattey 2010). However, some of these approaches used to transform RGB colour space are experiential relationships and it is not always easy to distinguish the vegetation from background.

Different colour spaces (RGB, CIE $L^*a^*b^*$ and i1i2i3 colour spaces) were compared to determine which was best for separating the vegetated from the non-vegetated portions of digital colour photographs. The CIE $L^*a^*b^*$ (abbreviated as $L^*a^*b^*$) colour space is an international standard for colour measurements, adopted by the Commission Internationale d'Eclairage (CIE) in 1976. L^* is the luminance or lightness component, parameter a^* defines the content of red or green, and parameter b* defines the yellow or blue content (Yam & Papadakis 2004). $L^*a^*b^*$ colour space is very close to the human perception of colour. Another advantage of this colour space is that the correlations between the channels are minimal in comparison to RGB because the brightness of the digital image is separated from the a^* and b^* dimensions to form the L^* dimension. The a^* channel is recommended for green vegetation detection. Theoretically, negative a^* values indicate green, while positive a^* values indicate red; however, the threshold of the a^* dimension is typically negative. This may be a result of shooting conditions, such as scatter from the blue-green sky or the vegetation types present. An equation (Philipp & Rath 2002) was introduced to transform the images from RGB to i1i2i3 colour space.

Next, a distance index was incorporated to evaluate the separability between vegetated and non-vegetated portions of the digital images, as follows:

$$\mathrm{SDI} = \frac{|\mu_1 - \mu_2|}{\sigma_1 + \sigma_2} \qquad (2)$$

where SDI is the separability distance index, μ_1 and μ_2 are the means, and σ_1 and σ_2 are the standard deviations of the green vegetation and the background, respectively. SDI is valid when distributions are Gaussian or near Gaussian.

Table 1 shows the separability distance indices for 12 RGB images that have been transformed to $L^*a^*b^*$ and i1i2i3 colour spaces. The larger the SDI, the easier it is to separate vegetation from non-vegetated background; thus, for all except images 9, 10 and 12, $L^*a^*b^*$ colour space makes it easier to separate vegetation from non-vegetation.

Figure 2 shows the distributions of a^* for the compared 12 images mentioned above. From Fig. 2 and after processing a large number of in situ digital images using visual estimations, we concluded that the thresholds of the a^*

Doi: 10.1111/j.1654-1103.2011.01373.x

Table 1. Separability distance index for images in three color spaces.

Images	RGB (2G−R−B)	$L^*a^*b^*$ (a^*)	i1i2i3 (i3)
1	0.037	0.380	0.148
2	0.071	0.321	0.286
3	0.039	0.353	0.158
4	0.028	0.156	0.115
5	0.000	0.238	0.000
6	0.024	0.137	0.096
7	0.015	0.622	0.367
8	0.070	0.580	0.280
9	0.208	0.077	0.834
10	0.087	0.330	0.348
11	0.029	0.276	0.114
12	0.031	0.073	0.348

dimension in the $L^*a^*b^*$ colour space always fall at less than 0. This rather arbitrary way of setting a possible range appears to work well in practice; however, other image processing techniques for determining the threshold can also be applied.

Setting thresholds

As described above and in Eq. (1), two Gaussian distribution models were used to interpret the distribution of the a^* dimension in $L^*a^*b^*$ colour space. Also, two methods were employed to determine a more accurate threshold value, T, which is used to segment the digital images. The first method (which we call the T_1 thresholding method) sets functions in Eq. (1) equal to each other, and sets the optimum threshold where the curves for the objective distribution and background distribution curves intersect (Fig. 3a). In this case, the total commission error (or omission error) of the vegetation segment and the non-vegetation background (represented by the total area of S_1 and S_2 in Fig. 3a) is minimal. The following equations are used

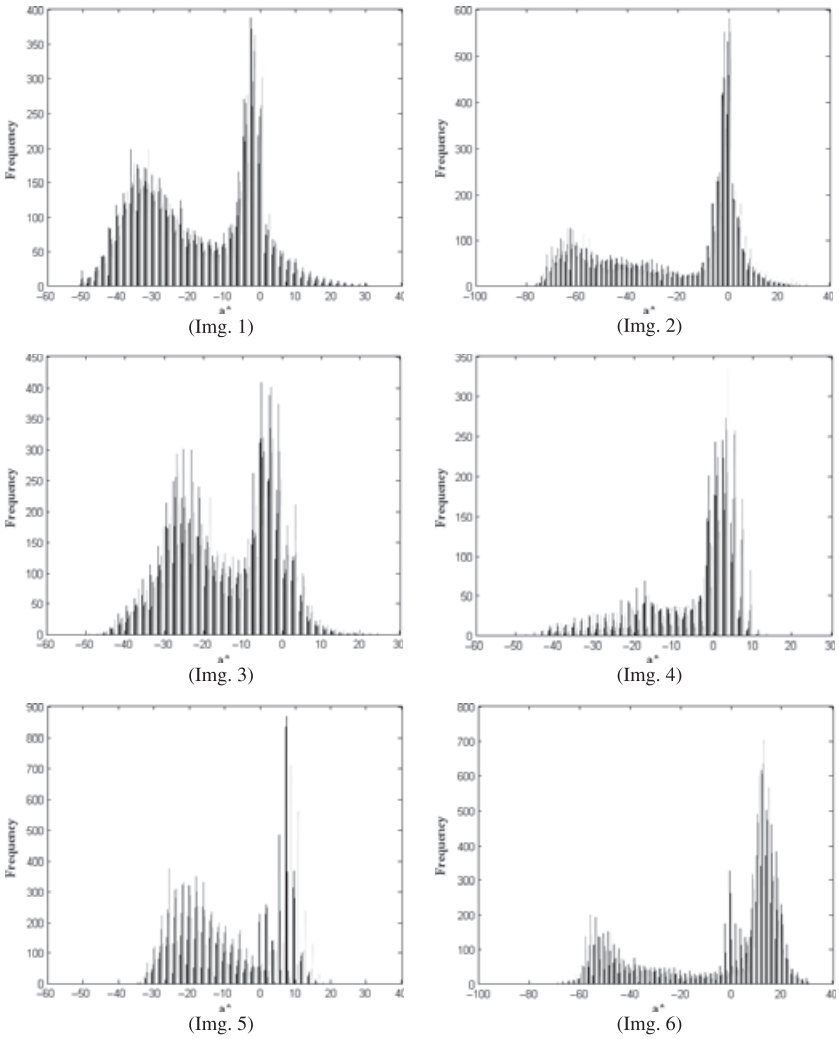

Fig. 2. Distributions of the a^* for 12 images (Img. 1–Img. 12).

Doi: 10.1111/j.1654-1103.2011.01373.x

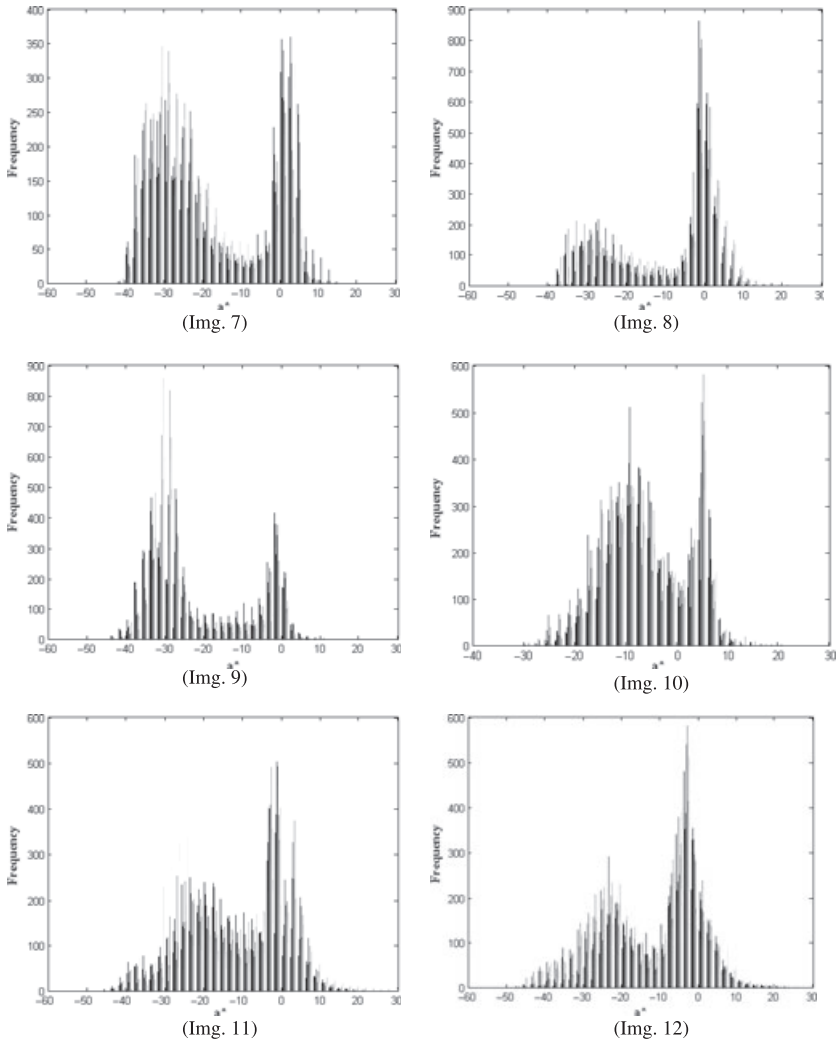

Fig. 2. (*Contiuned*)

for solving the threshold T_1 (when functions in Eq. (1) are equal to each other) (Gonzalez et al. 2002):

$$AT^2 + BT + C = 0 \tag{3}$$

where,

$$\begin{cases} A = \sigma_1^2 - \sigma_2^2 \\ B = 2(\mu_1\sigma_2^2 - \mu_2\sigma_1^2) \\ C = \sigma_1^2\mu_2^2 - \sigma_2^2\mu_1^2 + 2\sigma_1^2 2\sigma_2^2\, ln(\sigma_2\omega_1/\sigma_1\omega_2) \end{cases} \tag{4}$$

In this situation, the solution for T_1, which falls at the intersection of the two curves, is as follows:

$$T_1 = \frac{-B \pm \sqrt{B^2 - 4AC}}{2A} \tag{5}$$

If the variances are equal (i.e. $\sigma^2 = \sigma_1^2 = \sigma_2^2$), a single threshold is sufficient, as shown below in Eq. (7) (Gonzalez & Woods 2002):

$$T_1 = \frac{\mu_1 + \mu_2}{2} + \frac{\sigma^2}{\mu_1 - \mu_2} ln(\omega_1/\omega_2) \tag{6}$$

Another method, which we call the T_2 thresholding method, is based on the idea that the misclassification probability of the object and background are equal. This strategy is expected to lead to an unbiased estimate of FVC. A complementary error function is incorporated to find the threshold:

$$erfc(x) = 1 - erf(x) = \frac{2}{\sqrt{\pi}} \int_x^{\infty} e^{-t^2} dt \tag{7}$$

Doi: 10.1111/j.1654-1103.2011.01373.x

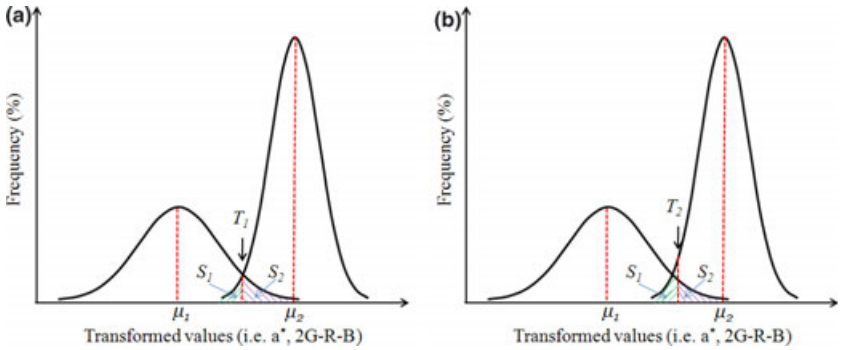

Fig. 3. The T_1 and T_2 methods for determining the threshold for image segmentation: (a) T_1 represents the point at which the two curves intersect and the total error of commission (or omission) is minimal; (b) T_2 represents the point at which the classification error for the object (vegetation) is equal to that for the background and is based on the assumption that the probability of misclassification of either object or background is equivalent.

When the classification error of the object is equal to the error of the background (i.e. the area of S_1 is equal to the area of S_2 in Fig. 3b), the optimal threshold T_2 is represented as:

$$w_1 \cdot erfc(\frac{x-\mu_1}{\sqrt{2}\sigma_1}) = w_2 \cdot erfc(\frac{\mu_2 - x}{\sqrt{2}\sigma_2}) \quad (8)$$

Extracting green fractional vegetation cover from digital images

Figure 4 is a flow chart that describes the extraction process. First, the digital image were converted from RGB colour space to $L^*a^*b^*$ colour space. Assuming that the distribution of a^* is Gaussian, the vegetation was separated from the non-vegetated background using an initial threshold T_0 and two Gaussian models were used to fit the vegetation and non-vegetation of the a^* dimension. Next, the optimal threshold was selected using one of the two methods (T_1 or T_2 thresholding method). The selected threshold, T, was then used to segment the digital images and calculate the green vegetation cover.

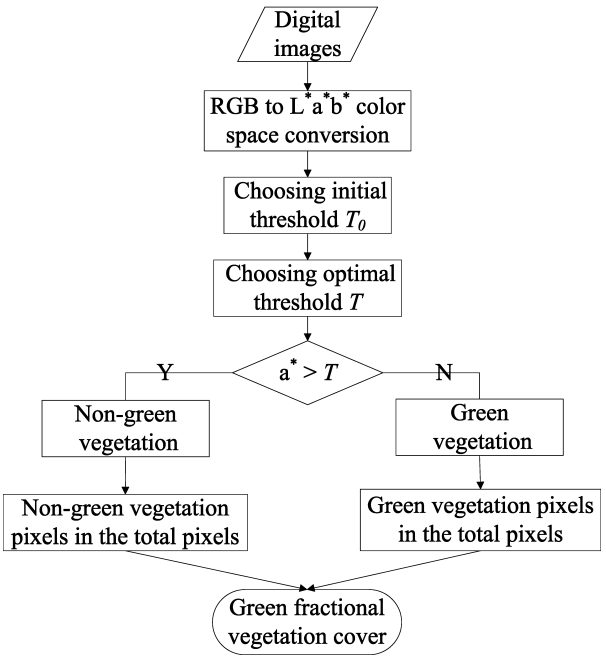

Fig. 4. Flow chart illustrating the extraction of FVC from digital images.

In extreme situations where images contain only one component (e.g. all vegetation or all bare soil, as shown in Fig. 5), an experiential threshold was used to calculate the fractional green vegetation cover. Although calculating the fractional green vegetation cover for an image containing 100% or zero vegetation is easy, we advise using a robust and automatic algorithm for these situations. The first step is to determine whether the image contains: (1) all vegetation; (2) all bare soil; or (3) a mixture of the two. The detailed process for identifying the optimal threshold T under these three conditions is shown in Fig. 6 and described by the following equations:

$$\text{Condition (1)} \ \frac{max(|\mu_1|,|\mu_2|)}{min(|\mu_1|,|\mu_2|)} < 3 \ \& \ \mu_1 < -2 \ \& \ \mu_2 < -2 \quad (9)$$

$$\text{Condition (2)} \ \frac{max(|\mu_1|,|\mu_2|)}{min(|\mu_1|,|\mu_2|)} < 3 \ \& \ \mu_1 > -2 \ \& \ \mu_2 > -2 \quad (10)$$

$$\text{Condition (3)} \ min(\mu_1,\mu_2) < x < max(\mu_1,\mu_2) \quad (11)$$

$$T' = \frac{\mu_1+\mu_2}{2} + \frac{\mu_1\sigma_1 + \mu_2\sigma_2}{\mu_1 - \mu_2} ln(\frac{\omega_1}{\omega_2}) \quad (12)$$

According to the designed algorithm, the MATLAB® software program (MathWorks, Inc., Natick, MA, USA)

Doi: 10.1111/j.1654-1103.2011.01373.x

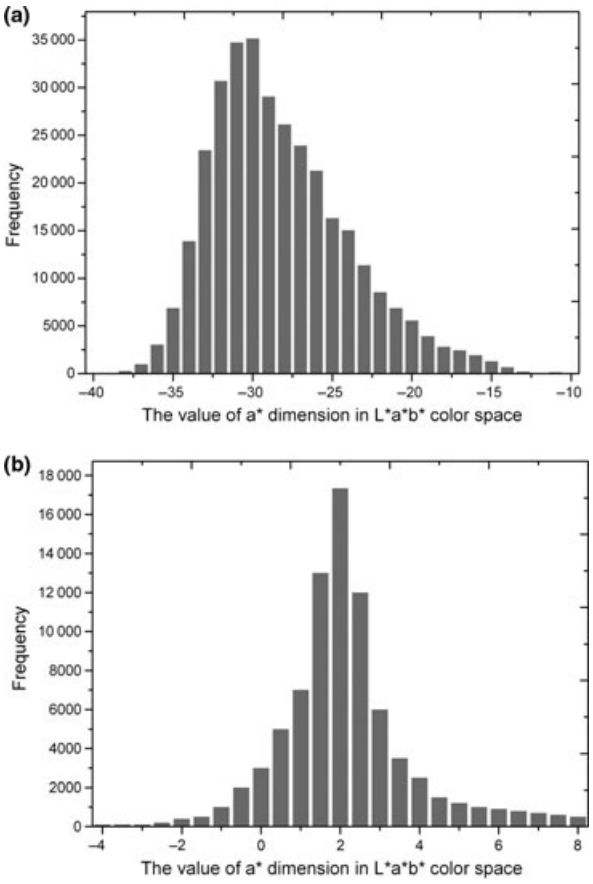

Fig. 5. Extreme distributions for the a^* component of digital images, showing (**a**) a photograph containing only green vegetation and (**b**) a photograph of bare soil.

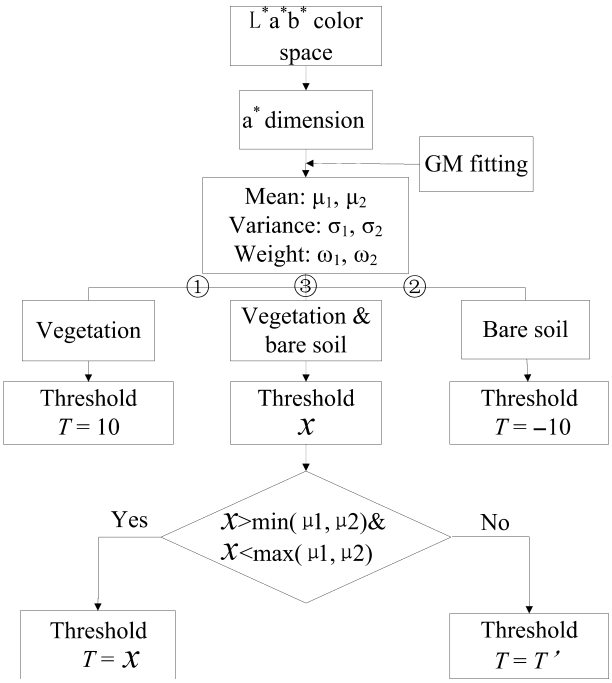

Fig. 6. Flow chart showing the method for determining the optimal threshold for segmentation.

was adapted to incorporate this algorithm through a user-friendly interface. The system segments digital images automatically and thus can extract fractional green vegetation covers quickly with no man–machine interaction.

Results

The main difficulty in evaluating methods for estimating vegetation cover is that the actual FVC is not known. We tested our algorithm using two approaches: (1) using a simulated picture in which the actual FVC is known; and (2) a cross-validation of several methods using the same field-measured data sets.

Analysis and evaluation based on simulated data

We validated our proposed algorithm using a simulated image that was 366 by 366 pixels, and contained several green mosaics (see Fig. 6). All the mosaics and background were subsets of vegetation and bare soil in real pictures. These pictures were captured in different light conditions; hence the colours of leaves and bare soil varied highly in the synthetic image. The green FVC of the simulated image has an accuracy of 0.426. We extracted the fractional green vegetation cover from the simulated picture using four approaches: (1) our proposed method (with thresholding method T_0); (2) a supervised classification (using the maximum likelihood method in ENVI software); (3) an unsupervised classification (using the ISODATA method in ENVI software), and the 2G−R−B method (Liu & Pattey 2010).

Figure 7 shows the results of the above test. The result using our method (with thresholding method T_0) is 0.436, which correlate well to the actual FVC. While results using the supervised classification, unsupervised classification and 2G−R−B (Liu & Pattey 2010) methods are 0.484, 0.523 and 0.478, respectively.

Analysis and evaluation based on digital images from field experiments

The FVC of several different vegetation types was extracted from the digital images automatically using our two proposed methods of threshold determination (T_1 and T_2). It is interesting to note that the extracted FVC with the initial threshold (T_0) compared well to the extracted images using

Doi: 10.1111/j.1654-1103.2011.01373.x

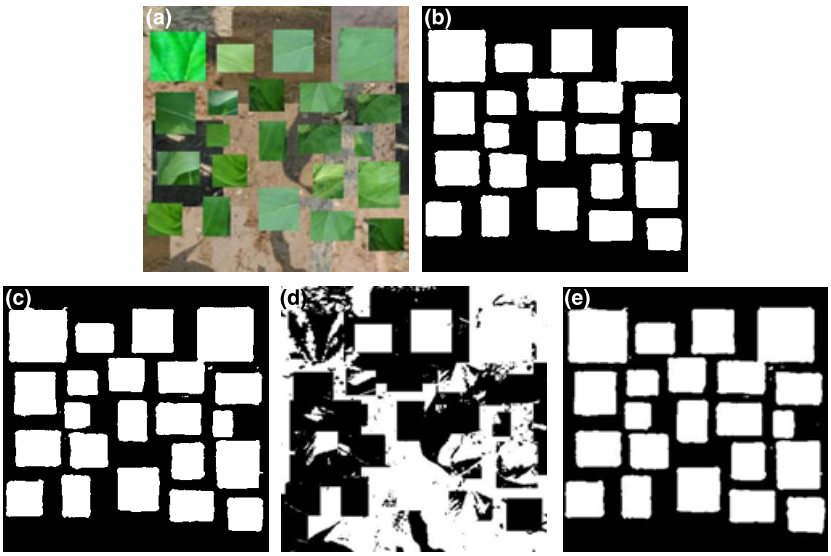

Fig. 7. Segmentation of simulated image using various methods: (**a**) the original simulated image with a FVC of 0.426, (**b**) segmentation using the new algorithm with a computed FVC of 0.436, (**c**) segmentation using the supervised classification method with a FVC of 0.484, (**d**) segmentation using the unsupervised classification method with a FVC of 0.523, and (**e**) segmentation using the 2G−R−B (Liu & Pattey 2010) method with a FVC of 0.478.

the T_1 and T_2 methods. To double-check our classification accuracy assessment, we also estimated the FVC with a method described in Liu & Pattey (2010), which uses 2G−R−B greenness space, a supervised classification method, and an unsupervised classification method. The results of this cross validation are shown in Fig. 8 and Table 2 for three vegetation types (maize, peanut and grapevine).

The supervised classification method relies on the training samples selected to classify objects, and inappropriate or poorly matched data may cause results to deviate from reality. In Fig. 8, the supervised method tends to overestimate the FVC for peanuts and underestimate it for grapevine, when compared to the other results, although the differences seem trivial. As judged by visual interpretation, most of the disputed areas are found on shaded leaves. This is due to confusion between dark-green shaded leaves and other shaded background elements (Liu & Pattey 2010).

To quantitatively evaluate the accuracy of our methods, we used the error index described below:

$$\sigma = \frac{\sum \frac{|\mathrm{FVC}_{extracted} - \mathrm{FVC}_{actual}|}{\mathrm{FVC}_{actual}}}{N} \qquad (10)$$

where $\mathrm{FVC}_{\mathrm{extracted}}$ is the extracted FVC from the classification methods, $\mathrm{FVC}_{\mathrm{actual}}$ is the extracted FVC from the supervised classification method, and N is the number of tested images. Table 2 shows the FVC of various vegetation types and the mean associated errors for the methods (three variations): the reference method using 2G−R−B greenness (Liu & Pattey 2010), the unsupervised classification method, and the supervised classification method. The errors for the different methods are less than 0.04, with exception of the unsupervised method, which has an error of 0.2933.

Plant leaves may vary from greyish-green to deep-green, and thus vegetation can cover a wide range of the a^* component of the $L^*a^*b^*$ colour space. In general, the distribution of vegetation, as represented in a histogram, is more dispersed than that of soil. As a result, the probability of misclassifying vegetation as non-vegetation is greater than that of misclassifying soil as vegetation, corresponding to Fig. 3a where S_2 is larger than S_1. Consequently, the FVCs obtained with the T_2 threshold strategy are generally greater than those provided from the T_1 strategy. Pear is the one exception to this, because its vegetation shows less variance than that of the non-vegetated areas of the images.

The mean errors associated with the FVC values provided with our approach and the supervised classification method are less than 0.035, which is close to the mean errors of FVC extracted with 2G−R−B (Liu & Pattey 2010) and the supervised classification method. Figure 9 shows a scatter plot of the FVC values extracted with our approach and the 2G−R−B method (Liu & Pattey 2010) against values obtained through the supervised classification method.

The selection of appropriate training samples for use with the supervised classification method (to separate vegetation from non-vegetation) is difficult. Factors such as leaf clumping, shadows and background noise contribute to the extraction error of FVC in the supervised method.

Doi: 10.1111/j.1654-1103.2011.01373.x

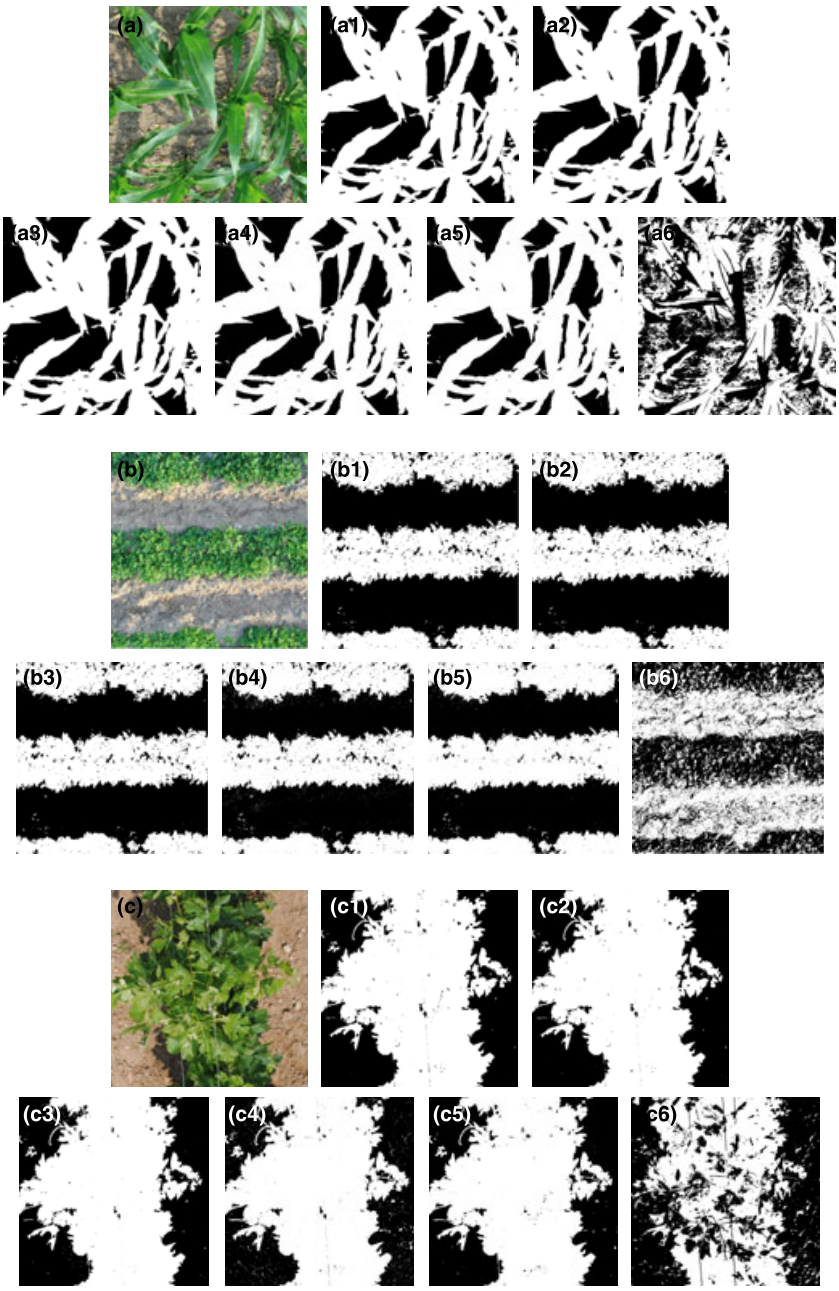

Fig. 8. Original digital colour images and their FVCs extracted with different methods. (**a–c**) are the original colour digital images of maize, peanut and grapevine; (**a1–c1**), (**a2–c2**), (**a3–c3**), (**a4–c4**) ,(**a5-c5**) and (**a6-c6**) are the corresponding segmentation results with our methods (T_0, T_1 and T_2 thresholding method), the method proposed in Liu et al. (2010) , supervised classification method and unsupervised classification method, respectively.

Our proposed approach has another advantage in that the thresholds can be adjusted automatically to detect vegetation more accurately under specific conditions, thus helping to remove residual effects related to shadows and other environmental conditions that affect image quality and FVC extraction accuracy. Figure 10 shows how our approach can be used to accurately extract the FVC from digital images obtained in the morning, at midday, in the afternoon and on cloudy day. Extractions were made from the original digital colour images using the T_2 thresholding method, which allowed adjustments to be made that helped filter out shadows and other

Journal of Vegetation Science
Doi: 10.1111/j.1654-1103.2011.01373.x

Table 2. Fractional vegetation cover of various vegetation types extracted with different methods.

Vegetation Type	Our Methods T_0	T_1	T_2	2G−R−B (Liu & Pattey 2010)	Unsupervised Classification	Supervised Classification
Maize	0.6352	06387	0.6425	0.6537	0.5797	0.6730
Peanut	0.4608	0.4608	0.4660	0.4754	0.5253	0.4839
Vine	0.5995	0.6064	0.6101	0.6311	0.4969	0.6134
Peach	0.6139	0.6139	0.6251	0.6354	0.3356	0.6520
Weeds	0.8300	0.8341	0.8405	0.8694	0.5816	0.8430
Pear	0.9191	0.9260	0.9191	0.9429	0.4100	0.9120
Mean Error (σ)	0.0347	0.0329	0.0233	0.0276	0.2933	–

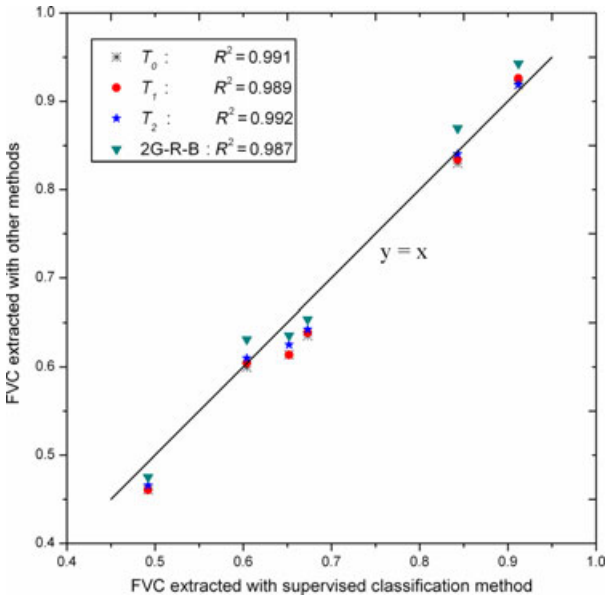

Fig. 9. Scattergram of FVCs extracted using the supervised classification method, our approach, and that of Liu & Pattey (2010).

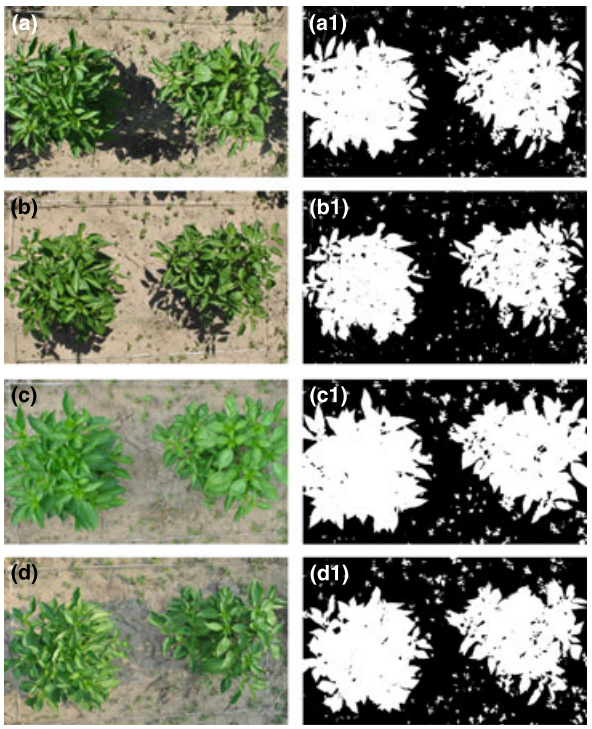

Fig. 10. Original digital colour images obtained at the same position under various conditions and the corresponding segmentation results with our proposed approach (T_2 thresholding). (**a**–**d**) The original colour digital images obtained in the morning (**a**), at midday with a very high sun (**b**), in the afternoon with a clear sky (**c**), and on a cloudy day with no sunlit leaves (**d**); (**a1**) to (**d1**) are the corresponding segmentation results.

interference. Figure 11 shows the distributions of a^* for the original photos obtained in different conditions.

Factors such as sunlit leaves and non-homogeneous illumination may affect the a^* distribution, which will influence the extraction of FVC. However, this error was not obvious in the tested results using our method. Shaded leaves affected the extraction more rather than sunlit leaves. This is because the sunlit leaves are more easily separated with the soil in the a^* dimension than the shaded leaves. Non-Gaussian distributions of the a^* component often occurred when there were more than two components in the image, i.e. shaded leaves, sunlit leaves and bare soil. In the case of a sunny midday, some non-Gaussian distributions existed (Fig. 11b), because the a^* values of shaded leaves were distributed between those of normal leaves and the background. Non-Gaussian shapes conflicted with the assumption of our methods. However, it should be noted that most shaded leaves were illuminated by scattered light; our methods tended to easily distinguish this shaded vegetation. Some extreme cases occurred in very black shaded leaves, at times of very weak light on the leaves. In this case, shaded leaves (or shaded soil, or other factors) were likely to be misclassified. Generally, and fortunately, the size of extremely black vegetation was generally smaller than that of a leaf, and occupied a very small fraction of the whole image.

Doi: 10.1111/j.1654-1103.2011.01373.x

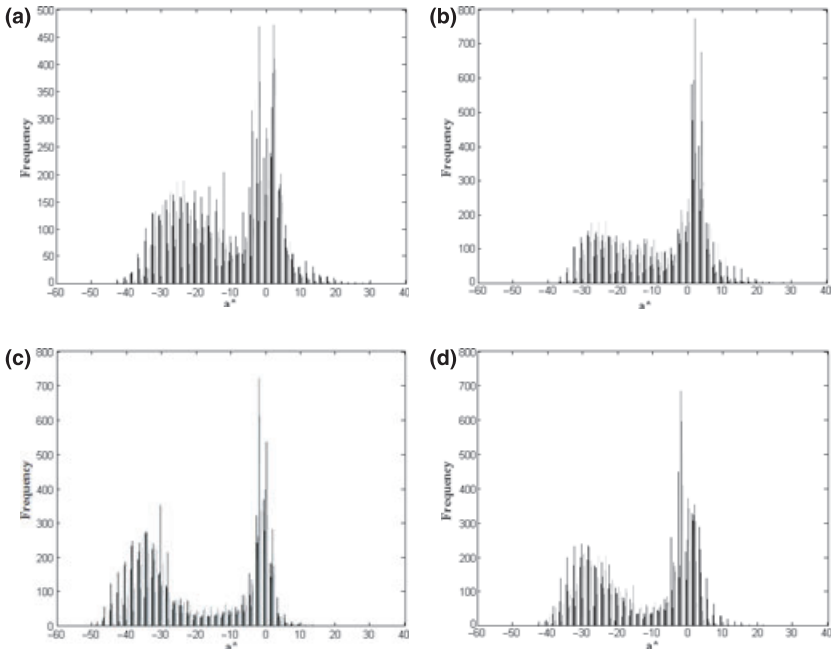

Fig. 11. Distributions of the a^* for the original photos obtained in different conditions (**a**–**d**): (**a**) original image obtained in the morning, (**b**) original image obtained at midday with very high sun, (**c**) original image obtained in the afternoon with a clear sky and, (**d**) original image obtained on a cloudy day with no sunlit leaves.

Under cloudy days, all leaves are shaded. This corresponds to an image only composed of two components. In Fig. 11d, two peaks can be seen clearly in the a^* distribution, which means that it is more likely to be segmented as vegetation and background, with little uncertainty.

Discussion

Remote sensing researchers recognize the need for field-measured FVC values to help establish quantitative FVC retrieval models. Digital photography is a popular approach for obtaining FVC measurements because it is more objective, accurate and reliable than other commonly used ground investigation methods due to the removal of subjectivity and human-introduced inconsistency (Brown et al. 2000; Zhou & Robson 2001). However, the efficiency of extracting green FVC from digital images is affected by two factors: whether the method can be automated and whether it classifies accurately.

We have presented a novel and practical method that facilitates FVC extraction from digital images. The results demonstrate that the $L^*a^*b^*$ colour space is optimal for this purpose and that the developed algorithm introduces three methods for determining the threshold for separating vegetation from background in the a^* dimension. The initial threshold, T_0, is selected by searching the a^* value with minimal frequency in an experiential range of less than 0. The threshold T_1 is selected by minimizing the total commission error; this threshold represents the intersection of the distribution curves for vegetation and background. The threshold T_2 is determined by setting the vegetation and background commission errors equal to each other. Although the initial threshold T_0 method has lower accuracy than the T_1 and T_2 methods, it is the simplest to implement and the results appeared acceptable in our validation test, probably because the $L^*a^*b^*$ colour space provides a large enough distance between the two classes. Generally, however, we recommend the use of the threshold T_2 method.

Our accuracy assessment indicates that the proposed approach performs as well as the method proposed in Liu & Pattey (2010), and is demonstrated to be feasible and applicable for extracting the FVC of different vegetation types with varying background and shadow conditions. We developed programs to apply our new algorithm, enabling segmentation to be executed automatically. This reduces the need for human–computer interaction to a minimum.

However, it should be noted that our algorithm design assumes a Gaussian distribution for both the vegetated and non-vegetated portions of a digital image. This assumption may be problematic when the algorithm is applied to more varied types of vegetation. The method should be further investigated, particularly with respect

Doi: 10.1111/j.1654-1103.2011.01373.x

to images that contain various vegetation types. Another potential issue is the impact of view angle effects on the images. We handled this issue by cropping the edges of the images used in this study, but more in-depth research will help to validate how this impacts the estimation of FVC.

Acknowledgements

This study was partially funded by the Major State Basic Research Development Program of China (ID: 2007CB714402), the seven project of the European Union Plan (ID: 212921), the Young Talent project (ID: 10QN-07) supported by the State Key Laboratory of Remote Sensing Science and the Specialized Research Fund for the Doctoral Program of Higher Education (SRFDP, ID: 20100003120020). We thank Dr. Jianggui Liu and Elizabeth Pattey for their kind assistance in extracting FVC from digital images with their GreenCropTracker tool. We appreciate help received from Jing Zhao, Xia Meng, Xiaobin Zhang and other team members in completing our field experiments. We also appreciate two anonymous reviewers for their comments and suggestions on an earlier version of the manuscript.

References

Adams, J.E. & Arkin, G.F. 1977. A light interception method for measuring row crop ground cover. *Soil Science Society of America Journal* 41: 789–792.

Andreasen, C., Rudemo, M. & Sevestre, S. 1997. Assessment of weed density at an early stage by use of image segmentation. *Weed Research* 37: 5–18.

Baret, F., Solan, B.de, Lopez-Lozano, R., Ma, K. & Weiss, M. 2010. GAI estimates of row crops from downward looking digital photos taken perpendicular to rows at 57.5° zenith angle: theoretical considerations based on 3D architecture models and application to wheat crops. *Agricultural and Forest Meteorology* 150: 1393–1401.

Behrenfeld, M.J., Randerson, J.T., McClain, C.R., Feldman, G.C., Los, S.O., Tucker, C.J., Falkowski, P.G., Field, C.B., Frouin, R., Esaias, W.E., Kolber, D.D. & Pollack, N.H. 2001. ENSO-scale variations in biospheric photosynthesis. *Science* 291: 2594–2597.

Booth, D.T., Cox, S.E., Meikle, T.W. & Fitzgerald, C. 2006. The accuracy of ground-cover measurements. *Rangeland Ecology and Management* 59: 179–188.

Brogaard, S. & Ólafsdóttir, R. 1997. Ground-truths or ground-lies? Environmental sampling for remote sensing application exemplified by vegetation cover data. Lund Electronic report in Physical Geography No. 1, October. Department of Physical Geography, Lund University. Sweden.

Brown, P.L., Doley, D. & Keenan, R.J. 2000. Estimating tree crown dimensions using digital analysis of vertical photographs. *Agricultural and Forest Meteorology* 100: 199–212.

Choudhury, B.J. 1994. Synergism of multispectral satellite observations for estimating regional land surface evaporation. *Remote Sensing of Environment* 49: 204–214.

Demarez, V., Duthoit, S., Baret, F., Weiss, M. & Dedieu, G. 2008. Estimation of leaf area and clumping indexes of crops with hemispherical photographs. *Agricultural and Forest Meteorology* 148: 644–655.

Dymond, J.R., Stephens, P.R., Newsome, P.F. & Wilde, R.H. 1992. Percentage vegetation cover of a degrading rangeland from SPOT. *International Journal of Remote Sensing* 13: 1999–2007.

Elvidge, C.D. & Chen, Z.K. 1995. Comparison of broad-band and narrow-band red and near-infrared vegetation indices. *Remote Sensing of Environment* 54: 38–48.

Gallegos, T.A. & Glimskar, A. 2009. Computer-aided calibration for visual estimation of vegetation cover. *Journal of Vegetation Science* 20: 973–983.

Gonzalez, R.C. & Woods, R.E. 2002. *Digital image processing: second edition*. Prentice Hall, Upper Saddle River, NJ, US, pp. 595–612.

Gower, S.T., Kucharik, C.J. & Norman, J.M. 1999. Direct and indirect estimation of leaf area index, fAPAR and net primary production of terrestrial ecosystems. *Remote Sensing of Environment* 70: 29–51.

Graham, E.A., Yuen, E.M., Robertson, G.F., Kaiser, W.J., Hamilton, M.P. & Rundel, P.W. 2009. Budburst and leaf area expansion measured with a novel mobile camera system and simple color thresholding. *Environmental and Experimental Botany* 65: 238–244.

Hoffmann, W.A. & Jackson, R. 2000. Vegetation–climate feedbacks in the conversion of tropical savanna to grassland. *Journal of Climate* 13: 1593–1602.

Kercher, S.M., Frieswyk, C.B. & Zedler, J.B. 2003. Effects of sampling teams and estimation methods on the assessment of plant cover. *Journal of Vegetation Science* 14: 899–906.

Leblanc, S.G., Chen, J., Fernandes, R., Deering, D.W. & Conley, A. 2005. Methodology comparison for canopy structure parameters extraction from digital hemispherical photography in boreal forests. *Agricultural and Forest Meteorology* 129: 187–207.

Liu, J.G. & Pattey, E. 2010. Retrieval of leaf area index from top-of-canopy digital photography over agricultural crops. *Agricultural and Forest Meteorology* 150: 1485–1490.

Louhaichi, M., Borman, M.M. & Johnson, E. 2001. Spatially located platform and aerial photography for documentation of grazing impacts on wheat. *Geocarto International* 16: 65–70.

Macfarlane, C., Hoffman, M., Eamus, D., Kerp, N., Higginson, S., McMurtrie, R. & Adams, M. 2007. Estimation of leaf area index in eucalypt forest using digital photography. *Agricultural and Forest Meteorology* 143: 176–188.

Doi: 10.1111/j.1654-1103.2011.01373.x

McVicar, T.R. & Jupp, D.L.B. 1998. The current and potential operational uses of remote sensing to aid decisions on drought exceptional circumstances in Australia: a review. *Agricultural Systems* 57: 399–468.

Nemani, R. & Running, S.W. 1996. Global vegetation cover changes from coarse resolution satellite data. *Journal of Geophysical Research* 101: 7157–7162.

Ohta, Y., Kanade, T. & Sakai, T. 1980. Colour information for region segmentation. *Computer Graphics and Image Processing* 13: 222–241.

Philipp, I. & Rath, T. 2002. Improving plant discrimination in image processing by use of different colour space transformations. *Computers and Electronics in Agriculture* 35: 1–15.

Prince, S.D. 1991. Satellite remote sensing of primary production: comparison of results for Sahelian grasslands 1981–1988. *International Journal of Remote Sensing* 12: 1301–1311.

Qi, J., Marsett, R.C., Moran, M.S., Goodrich, D.C., Heilman, P., Kerr, Y.H., Dedieu, G., Chehbounj, A. & Zhang, X.X. 2000. Spatial and temporal dynamics of vegetation in the San Pedro River basin area. *Agricultural and Forest Meteorology* 105: 55–68.

Schimel, D.S., House, J.I., Hibbard, K.A., Bousquet, P., Ciais, P., Peylin, P., Braswell, B. H., Apps, M. J., Baker, D., Bondeau, A., Canadell, J., Churkina, G., Cramer, W., Denning, A. S., Field, C. B., Friedlingstein, P., Goodale, C., Heimann,, M., Houghton, R. A., Melillo, J.M., Moore III, B., Murdiyarso, D., Noble, I., Pacala, S. W., Prentice, I. C., Raupach, M. R., Rayner, P. J., Scholes, R. J., Steffen, W. L. & Wirth, C. 2001. Recent patterns and mechanisms of carbon exchange by terrestrial ecosystems. *Nature* 414: 169–172.

Sellers, P.J., Dickinson, R.E., Randall, D.A., Betts, A.K., Hall, F.G., Berry, J.A., Collatz, G.J., Denning, A.S., Mooney, H.A., Nobre, C.A., Sato, N., Field, C.B. & Henderson-Sellers, A. 1997. Modeling the exchanges of energy, water and carbon between continents and the atmosphere. *Science* 275: 502–509.

Tueller, P.T. 1987. Remote sensing science applications in arid environments. *Remote Sensing of Environment* 23: 143–154.

Vittoz, P., Bayfield, N., Brooker, R., Elston, D.A., Duff, E.I., Theurillat, J.-P. & Guisan, A. 2010. Reproducibility of species lists, visual cover estimates and frequency methods for recording high-mountain vegetation. *Journal of Vegetation Science* 21: 1035–1047.

Wells, K.F. 1971. Measuring vegetation changes on fixed quadrats by vertical ground stereography. *Journal of Range Management* 24: 233–236.

Wimbush, D.J., Barrow, M.D. & Costin, A.B. 1967. Colour stereophotography for the measurement of vegetation. *Ecology* 48: 150–152.

Woebbecke, D.M., Meyer, G.E., Von Bargen, K. & Mortensen, D.A. 1995. Color indices for weed identification under various soil, residue and lighting conditions. *Transactions of the ASAE* 38: 259–269.

Yam, K.L. & Papadakis, S. 2004. A simple digital imaging method for measuring and analyzing color of food surfaces. *Journal of Food Engineering* 61: 137–142.

Zhou, Q. & Robson, M. 2001. Automated rangeland vegetation cover and density estimation using ground digital images and a spectral-contextual classifier. *International Journal of Remote Sensing* 22: 3457–3470.

Zhou, Q., Robson, M. & Pilesjö, P. 1998. On the ground estimation of vegetation cover in Australian rangelands. *International Journal of Remote Sensing* 19: 1815–1820.

Doi: 10.1111/j.1654-1103.2011.01373.x